Mechanistic Studies of CVD Metallization Processes: Reactions of Rhodium and Platinum β-Diketonate Complexes on Copper Surfaces

Elizabeth L. Crane, Yujian You, Ralph G. Nuzzo,* and Gregory S. Girolami*

Contribution from the School of Chemical Sciences and Frederick Seitz Materials Research Laboratory, University of Illinois at Urbana−Champaign, Urbana, Illinois, 61801

Received October 12, 1999

Abstract: The hexafluoroacetylacetonate complexes Rh(hfac)$(C_2H_4)_2$ and Pt(hfac)$_2$ are known to serve as chemical vapor deposition precursors to Rh and Pt thin films. In the absence of a reducing carrier gas, the depositions are surface-selective and occur preferentially on copper, but under these conditions, the metallization processes are unexpectedly inefficient relative to the rapid deposition of Pd on Cu seen for the palladium analogue Pd(hfac)$_2$. Mechanistic studies of the reactions of Rh(hfac)$(C_2H_4)_2$ and Pt(hfac)$_2$ on copper surfaces under ultrahigh vacuum conditions have now been performed in order to elucidate the factors responsible for the differences among these surface-selective metallization processes. The studies demonstrate that adsorption of the rhodium complex Rh(hfac)$(C_2H_4)_2$ on copper surfaces is accompanied by the loss of the coordinated ethylene groups, even at 100 K. At these low temperatures, the adsorbed Rh(hfac) fragments are oriented in several ways with respect to the surface. Heating the substrate above ∼150 K causes the hfac ligands to realign to a perpendicular orientation relative to the surface. The platinum precursor Pt(hfac)$_2$ adsorbs molecularly at 100 K with the molecular planes of the hfac ligands oriented parallel to the copper surface. Heating the substrate to temperatures above 150 K again results in a realignment of the hfac ligands to a perpendicular orientation. This reorientation is accompanied by a partial reduction of the Pt centers (as judged from shifts seen in X-ray photoelectron spectroscopy core level data), a result suggesting that the hfac ligands begin to dissociate from the platinum centers near 150 K. At temperatures above 220 K, the transfer of the hfac ligands from both complexes to the copper surface is complete, as signaled by the reduction of the metal centers to the zero-valent state. The copper-bound hfac ligands are further transformed upon heating, either reacting with copper surface atoms to yield Cu(hfac)$_2$ (which desorbs at temperatures above 250 K) or decomposing (with fragments desorbing above 350 K). The presence of platinum on the copper surface promotes the former reaction as judged by the appearance of a new reaction-limited desorption process for Cu(hfac)$_2$. The presence of rhodium on the copper surface does not promote the formation of Cu(hfac)$_2$, although autocatalysis is noted in the steady-state reactive scattering data. The inability of the Rh and Pt precursors to engage in a sustained transmetalation reaction with the copper surface is attributed to the slow interdiffusion of copper through the Rh/Cu and Pt/Cu alloys that are produced in the near-surface region.

Introduction

Metal−organic chemical vapor deposition (MOCVD) processes have become increasingly attractive industrially owing to their ability to effect conformal coverages of nonplanar substrates, the advantages that result from low deposition temperatures, and the potential for surface-selective deposition.[1−5] The chemical vapor deposition of platinum-group metals is of particular interest because these metals are good electrical conductors, highly inert chemically, and not prone to electromigration.[6−8] Thin films and alloys of rhodium and platinum, for example, are potentially useful as replacements for gold films as contact materials in microelectronic devices. Alloys are of particular interest because they can be used to combine favorable aspects of several metals (e.g., platinum for improved contact corrosion resistance and copper for conductivity). Perhaps more significant, though, are the envisioned uses of platinum metallization schemes in the microfabrication of integrated capacitor assemblies based on ferroelectric thin films of perovskites (e.g., lead zirconium titanate and related materials).[9] It is therefore timely that the chemical vapor deposition (CVD) of thin films of platinum metals has received increasing attention in the past few years.[10−19] To date, however, there have been few detailed studies of the surface chemistry of rhodium or platinum

(1) Kodas, T. T., Hampden-Smith, M. J. Eds. *The Chemistry of Metal CVD*; VCH: New York, 1994 and references therein.
(2) Spencer, J. T. *Prog. Inorg. Chem.* **1994**, *41*, 145−237.
(3) Jensen, K. F.; Kern W. In *Thin Film Processes II*; Vossen, J. L., Kern, W., Eds.; Academic: Boston, 1991; Chapter III-1.
(4) Jensen, K. F. In *Microelectronic Processing: Chemical Engineering Aspects*; (*Adv. Chem. Ser.* 221), Hess, D. W., Jensen, K. F., Eds.; Advances in Chemistry Series 221; American Chemical Society: Washington, DC, 1989, Chapter 5.
(5) Rubezhov, A. Z. *Plat. Met. Rev.* **1992**, *36*, 26−33.
(6) Jeon, N. L.; Lin, W.; Erhardt, M. K.; Girolami, G. S.; Nuzzo, R. G. *Langmuir* **1997**, *13*, 3833−3838.
(7) Jones, R. E.; Desu, S. B. *MRS Bull.* **1996**, *21*, 55−58.
(8) Lee, J. M.; Hwang, C. S.; Cho, H.-J.; Suk, C.-G.; Kim, H. J. *J. Electrochem. Soc.* **1998**, *145*, 1066−1069.
(9) Jeon, N. L.; Clem, P.; Jung, D. Y.; Lin, W.; Girolami, G. S.; Payne, D. A.; Nuzzo, R. G. *Adv. Mater.* **1997**, *9*, 891−895.
(10) Rand, M. J. *J. Electrochem. Soc.* **1973**, *120*, 686−693.
(11) Morabito, J. M.; Rand, M. J. *Thin Solid Films* **1974**, *22*, 293−303.
(12) Garrido-Suarez, C.; Braichotte, D.; van der Bergh, H. *Appl. Phys. A* **1988**, *46*, 285−290.
(13) Braichotte, D.; van der Bergh, H. *Appl. Phys. A* **1987**, *44*, 353−359.
(14) Gilgen, H. H.; Cacouris, T.; Shaw, P. S.; Krchnavek, R. R.; Osgood, R. M. *Appl. Phys. B* **1987**, *42*, 55−66.

10.1021/ja993653s CCC: $19.00
Published on Web 03/28/2000

coordination complexes[20,21] that are relevant to CVD processes and, to our knowledge, that discuss processes for depositing alloy thin film microstructures.

We have described elsewhere studies of bis(hexafluoroacetylacetonato)palladium(II), $Pd(hfac)_2$, as a CVD precursor to deposit palladium alloy thin films selectively on copper and iron substrates.[22−25] The mechanisms operating in the remarkably efficient Pd/Cu system are now understood in detail;[23,24] the overall reaction responsible for the surface selectivity is a redox transmetalation reaction in which the Pd^{II} precursor is reduced to Pd^0 (and Cu^0 is oxidized to Cu^{II}):

$$Pd(hfac)_2 + Cu \rightarrow Pd + Cu(hfac)_2$$

In an effort to determine whether other metal hfac complexes can react similarly with copper surfaces, and thus serve as potential surface-selective CVD precursors, we undertook an investigation of the surface-mediated thermolytic decomposition of the rhodium and platinum hfac complexes (hexafluoroacetylacetonato)bis(ethylene)rhodium(I), $Rh(hfac)(C_2H_4)_2$,[26] and bis(hexafluoroacetylacetonato)platinum(II), $Pt(hfac)_2$.[27] Interestingly, we find that neither of these precursors reacts with a copper substrate via a sustained redox transmetalation reaction comparable to that observed for the palladium compound, $Pd(hfac)_2$. To determine the factors responsible for the different efficiencies seen for the rhodium and platinum precursors, we have studied the reactions of $Rh(hfac)(C_2H_4)_2$ and $Pt(hfac)_2$ on copper surfaces under ultrahigh vacuum (UHV) conditions. The results of our investigations are described herein.

Experimental Section

The experiments were performed in three separate UHV chambers, each of which has been described previously.[28,29] The chamber used for the temperature-programmed reaction spectroscopy (TPRS) and reactive molecular beam-surface scattering studies has a base pressure of $\leq 2 \times 10^{-10}$ Torr. It is pumped with a liquid nitrogen-trapped 25 cm diameter diffusion pump (5000 L s^{-1}) as well as a 25 cm diameter cryopump (10 000 L s^{-1}). This chamber is equipped with two quadrupole mass spectrometers, each shrouded and differentially pumped by 30 L s^{-1} ion pumps. A single-pass cylindrical mirror analyzer with conical electron gun (PHI) was used to examine the surface composition of the sample by Auger electron spectroscopy (AES). An ion gun (PHI) was used for sputtering the sample with Ar^+. The pressures cited here, which were monitored with a UHV ionization gauge, are not corrected for sensitivity and therefore the reported adsorbate exposures are only approximate.

The exposures were made using an effusive molecular beam with a 200 μm source aperture.[29] The Cu(111) crystal face was held less than 1 cm from the source. For the reactive scattering experiments, the sample was also positioned within 5 mm of the mass spectrometer skimmer during the dosing process. The backing pressure behind the aperture was monitored with a capacitance manometer (MKS, 1 Torr full scale). The typical backing pressures were 1.2×10^{-3} Torr for $Rh(hfac)(C_2H_4)_2$ (generated by cooling the precursor to ~273 K) and 4×10^{-3} Torr for $Pt(hfac)_2$ (generated by heating the precursor to ~323 K). Before dosing was begun, the headspaces in the precursor reservoirs were evacuated with a turbomolecular pump (520 L s^{-1}) to remove any volatile species that might have accumulated owing to decomposition of the precursors.

The reflection−absorption infrared (RAIR) spectra were taken in a turbomolecularly pumped (520 L s^{-1}) chamber equipped with an effusive molecular beam doser, a single-pass cylindrical mirror analyzer for AES, and a differentially pumped quadrupole mass spectrometer. The RAIR spectra were collected with a Digilab FTS 60A spectrometer and a wide-band MCT detector in conjunction with external reflection optics. These optics, maximized for single grazing angle reflection (~84°), are similar to those described elsewhere.[30] Dosing was performed from the background at pressures between 5×10^{-8} and 2×10^{-7} Torr. The single-beam spectrum of the clean substrate surface was used as a reference. The RAIR spectra were recorded in 1064 scans at a resolution of 4 cm^{-1}. The data are presented as absorbance plots ($-\log R/R_o$). RAIR spectra were recorded after the sample had been annealed at the indicated temperature for several seconds and then cooled to the temperature noted.

For both the TPRS and the RAIRS experiments, the Cu(111) single crystals were strapped to button heaters with tantalum support wires passed through notches in the sides of the substrate. The temperature was controlled with a Eurotherm temperature controller and monitored with a chromel−alumel thermocouple, which was lodged in a hole spark-cut in the side of the crystal. The crystals could be cooled and heated within the temperatures range 100−950 K; the typical heating rate was in the range of 1−5 K s^{-1}. The crystals were cleaned by sputtering with 1 keV Ar^+ ions for 15 min at 950 K and then annealed for 15 min at 950 K.

The X-ray photoelectron spectroscopy (XPS) experiments were performed in an ion-pumped chamber (240 L s^{-1}) equipped with a single-pass cylindrical mirror analyzer for AES, an SSL M-probe X-ray photoelectron spectrometer (Al Kα monochromatic source at 1487 eV), a PRI rear view four-grid low-energy electron diffractometer (LEED), and an ion sputtering gun. The polycrystalline copper foil used in the XPS experiments was fixed on a high-purity, oxygen-free Cu mounting stage which could be heated or cooled between 110 and 800 K; the maximum heating rate achievable was 2 K s^{-1}. A chromel−alumel thermocouple was located inside the copper block. The substrate was introduced into the chamber by means of a differentially pumped sample transfer rod. Dosing was controlled with a precision leak valve. The sample reservoirs containing $Rh(hfac)(C_2H_4)_2$ or $Pt(hfac)_2$ were kept at room temperature. Multilayers and saturation monolayers were generated by direct dosing using an effusive molecular beam source located ~1 cm from the sample surface. Submonolayers were generated by dosing from the background. XPS data were collected after the exposed copper surface had been annealed at the desired temperature for 15 min (Rh experiments), or for several seconds (Pt experiments), and then cooled to 120 or 300 K as indicated. The different anneal times reflect differences in the heat capacities of the hot stages used.

The secondary electrons generated during an XPS experiment can induce decomposition of the adsorbates. To determine the extent of damage caused during a typical analysis, a copper surface was saturated with $Rh(hfac)(C_2H_4)_2$ at room temperature and then XP spectra were collected as a function of an increasing exposure to the X-ray beam. Although there was no apparent change in the rhodium or copper XPS signals, the C 1s XPS spectrum changed significantly over 1 h. The

(15) Gozum, J. E.; Rogers, D. M.; Jensen, J. A.; Girolami, G. S. *J. Am. Chem. Soc.* **1988**, *110*, 2688−2689.
(16) Xue, Z.; Strouse, M. J.; Shuh, D. K.; Knobler, C. B.; Kaesz, H. D.; Hicks, R. F.; Williams, R. S. *J. Am. Chem. Soc.* **1989**, *111*, 8779−8784.
(17) Dryden, N. H.; Kumar, R.; Ou, E.; Rashidi, M.; Roy, S.; Norton, P. R.; Puddephatt, R. J. *Chem. Mater.* **1991**, *3*, 677−685.
(18) Xue, Z.; Thridandam, H.; Kaesz, H. D.; Hicks, R. F. *Chem. Mater.* **1992**, *4*, 162−166.
(19) Dossi, C.; Psaro, R.; Bartsch, A.; Brivio, E.; Galasco, A.; Losi, P. *Catal. Today* **1993**, *17*, 527−535.
(20) Igumenov, I. K. *J. Phys. IV* **1995**, *5*, C5/489−C5/496.
(21) Fusy, J.; Menaucourt, J.; Alnot, M.; Huguet, C.; Ehrhardt, J. J. *Appl. Surf. Sci.* **1996**, *93*, 211−220.
(22) Lin, W.; Warren, T. H.; Nuzzo, R. G.; Girolami, G. S. *J. Am. Chem. Soc.* **1993**, *115*, 11644.
(23) Lin, W.; Wiegand, B. C.; Nuzzo, R. G.; Girolami, G. S. *J. Am. Chem. Soc.* **1996**, *118*, 5977−5987.
(24) Lin, W.; Nuzzo, R. G.; Girolami, G. S. *J. Am. Chem. Soc.* **1996**, *118*, 5988−5996.
(25) Lin, W.; Warren, T. H.; Wilson, S. R.; Girolami, G. S., submitted for publication.
(26) Lin, W.; Girolami, G. S., in preparation.
(27) You, Y.; Girolami, G. S., in preparation.
(28) Hostetler, M. J.; Nuzzo, R. G.; Girolami, G. S.; Dubois, L. H. *J. Phys. Chem.* **1994**, *98*, 2952−2962.
(29) Bent, B. E.; Nuzzo, R. G.; Dubois, L. H. *J. Am. Chem. Soc.* **1989**, *111*, 1634−1644.
(30) See, for example: Nuzzo, R. G.; Zegarski, B. R.; Korenic, E. M.; Dubois, L. H. *J. Phys. Chem.* **1992**, *96*, 1355−1361.

peak near 292 eV due to the CF_3 carbon decreased in intensity and eventually disappeared. Similarly, the F 1s signal also gradually diminished and disappeared. These results indicate that the $C-CF_3$ functions in the hfac group are degraded by prolonged exposure to the X-rays. To minimize these effects, the XPS data were collected over total period of ~50 min in the following order: C 1s, F 1s, O 1s, Rh 3d, and Cu 2p. For the experiments using $Pt(hfac)_2$ the order used was C 1s, O 1s, F 1s, Cu 2p, Pt 4d, and Pt 4f. Variable-temperature spectra were each acquired from a freshly cleaned and dosed surface.

The $Rh(hfac)(C_2H_4)$[31] and $Pt(hfac)_2$ [32] precursors were synthesized according to literature procedures.

Results

In the following sections, we describe the chemistry of two platinum−metal hexafluoroacetylacetonate complexes, $Rh(hfac)(C_2H_4)_2$ and $Pt(hfac)_2$, on a Cu(111) substrate in an effort to understand the behavior seen for these precursors under CVD conditions. Several issues will be addressed: the identity and molecular organization of the species formed upon adsorption of the precursors on Cu(111) at low temperatures, the evolution of the surface-bound hfac ligand orientations at higher temperatures, the energetics involved in the dissociation of the ligands from the metal centers, the factors that affect the competition between ligand fragmentation reactions and the transmetalation reaction that leads to the formation of $Cu(hfac)_2$ via reactive etching, and the effect of metallic interdiffusion rates and alloy formation on the chemistry that occurs at the surface. We will present the results sequentially, beginning with studies of the reactivity patterns evidenced by $Rh(hfac)(C_2H_4)_2$ and followed by comparable studies of $Pt(hfac)_2$.

TPRS Studies of $Rh(hfac)(C_2H_4)_2$ on Cu(111). The adsorption and thermolytic decomposition of $Rh(hfac)(C_2H_4)_2$ on Cu(111) were examined by temperature-programmed reaction spectroscopy. The masses examined in this study were 26 (C_2H_2, which is the principal ethylene fragment, Figure 1a),[33] 28 ($C_2H_4^+$ and $CO,^+$ the latter being a fragment of the hfac group, Figure 1b), and 69 (CF_3^+ and $C_3O_2H^+$, which are also fragments of hfac, Figure 1c).[23] In addition, masses 103 (Figure 1d) and 63 (Figure 2) were followed to monitor the evolution of Rh- and Cu-containing products, respectively. For the data shown in Figure 1, exposures slightly exceeding a saturation monolayer were used (1.1−1.5 Θ_{sat}).

The mass 26 trace contains three desorption peaks at 160, 175, and 220 K; no ethylene desorption occurs above 300 K. TPRS traces taken as a function of exposure clearly show that the peak at 220 K corresponds to the desorption of intact $Rh(hfac)(C_2H_4)_2$ molecules from a multilayer (peaks at 220 K in the other mass channels are assigned to this same process). Two low-temperature peaks are also seen at 160 and 175 K. We assign these two low-temperature TPRS features to the desorption of the ethylene from (predominantly) the copper surface, because similar desorption temperatures have been seen by Bent et al. for ethylene on Cu(110).[34] Only ethylene desorbs at these temperatures, as shown by the absence of corresponding peaks in the traces that track desorption of hfac (mass 69) and Rh (mass 103). This result suggests that the adsorbed $Rh(hfac)(C_2H_4)_2$ molecules readily transfer their ethylene ligands to the Cu surface. At higher exposures of the precursor, this ethylene is progressively displaced from the Cu(111) surface, leading to the loss of these TPRS features.

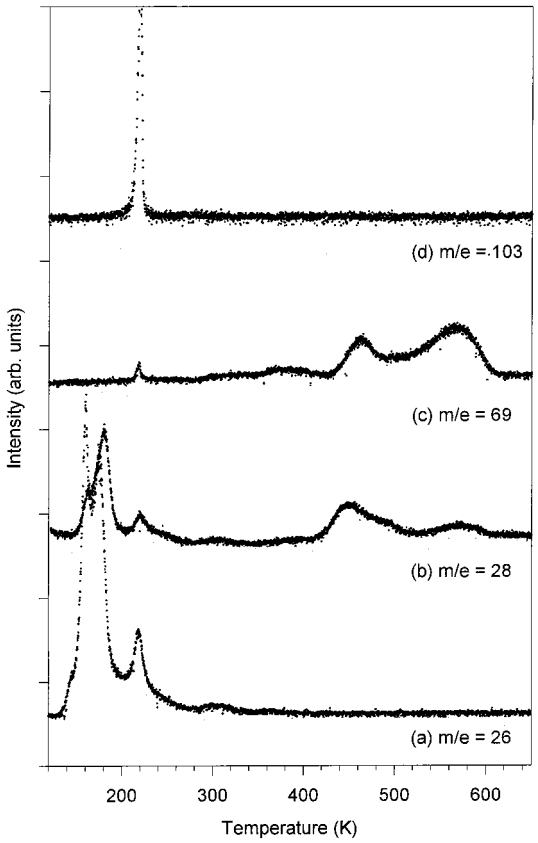

Figure 1. TPR spectra of multilayer quantity (1.1−1.5 Θ_{sat}) of $Rh(hfac)(C_2H_4)_2$ on Cu(111) dosed at 120 K. The masses followed were $m/e = 26$ (C_2H_2), $m/e = 28$ (C_2H_4 and CO), $m/e = 69$ (CF_3 and C_3O_2H), and $m/e = 103$ (Rh), as indicated in the figure.

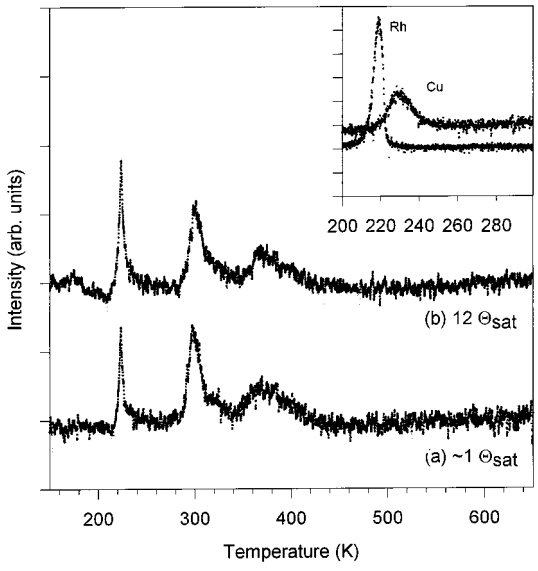

Figure 2. TPR spectra of multilayer quantity of $Rh(hfac)(C_2H_4)_2$ on Cu(111) dosed at 120 K. The mass followed was $m/e = 63$ (Cu) for the indicated doses. The inset shows the two metal desorption profiles.

The mass 28 trace (which tracks desorption of both ethylene and CO) also shows three peaks at 160, 175, and 220 K. We again assign the first two of these peaks to desorption of ethylene from the copper surface, and the latter peak to desorption of intact $Rh(hfac)(C_2H_4)_2$ molecules from a multilayer. The relative intensities of the three peaks are different from those in the mass

(31) Aneja, R.; Golding, B. T.; Pierpoint, C. *J. Chem. Soc., Dalton Trans.* **1984**, 219−224.
(32) Okeya, S.; Kawaguchi, S. *Inorg. Synth.* **1982**, *20*, 65−69.
(33) *Eight Peak Index of Mass Spectra*, 3rd ed.; Royal Society of Chemistry: London, 1983.
(34) Jenks, C. J.; Bent, B. E.; Bernstein, N.; Zaera, F. *Surf. Sci. Lett.* **1992**, *227*, L89−L94.

26 trace because slightly different exposures were used in the two experiments (see above).

The results above suggest that, by 220 K, the surface is decorated with Rh(hfac) units generated by dissociation (and subsequent desorption) of the ethylene ligands from the precursor.

At temperatures above 400 K, the TPRS traces show features that correspond to fragmentation of the hfac groups. The complex patterns seen between 400 and 600 K for mass 28 and mass 69 traces (Figure 1b and c) are in good agreement with those reported for the thermolysis of the hfac ligand on Cu(111).[23,35]

TPR spectra were also obtained for metal-containing fragments. Figure 1d shows the desorption profile seen at mass 103, which tracks desorption of Rh-containing species. Only one feature is seen here, that of the multilayer desorption at ~220 K. This desorption process has a temperature and coverage dependence (data not shown) characteristic of a zero-order rate law, as expected for desorption from a physisorbed multilayer.[36]

Most interesting were the TPRS traces seen at mass 63 (Figure 2). At coverages near a saturation monolayer (Figure 2a), three peaks were seen: at 230, 300, and 370 K. Although the first of these peaks occurs at a temperature similar to that for desorption of intact Rh(hfac)$(C_2H_4)_2$ molecules from the multilayer, the inset in Figure 2 clearly rules out the possibility that 230 K peak is due to the same process. Instead, we believe that the mass 63 channel, which corresponds to one of the isotopes of copper, tracks desorption of a new species, Cu(hfac)$_2$; when a Cu(111) surface is dosed with Cu(hfac)$_2$, a similar desorption feature is seen. Greatly increasing the Rh(hfac)$(C_2H_4)_2$ exposure (Figure 2b, $\Theta \cong 12\ \Theta_{sat}$) does not significantly change the yield of the Cu-containing product(s). This result suggests that moderate exposures are sufficient to saturate the reaction sites that produce the Cu-containing product. The low temperature of this (likely) Cu(hfac)$_2$ desorption process strongly implies that the surface-bound hfac ligands, which are derived from the Rh(hfac)$(C_2H_4)_2$ precursor, can etch the Cu surface at temperatures below 230 K. We emphasize, however, that the yield of this Cu-containing product is low.

Whereas the 230 K feature in the mass 63 trace is assigned to a desorption-limited process, the higher temperature peaks at 300 and 370 K are assigned to reaction-limited desorption of Cu(hfac)$_2$. Again, similar peaks are seen when Cu(hfac)$_2$ is dosed on a Cu(111) substrate (such processes have not been reported in the literature by others examining this latter system).[35] The amount of Cu(hfac)$_2$ produced in these reaction-limited processes is again relatively small and sensitive to the sample history. Figure 3 shows the results of experiments in which an initially clean and annealed copper surface was treated as follows: (1) the surface was dosed with either 4.0 or 8.0 θ_{sat} of Rh(hfac)$(C_2H_4)_2$ at 120 K, (2) the surface was ramped to a set temperature, (3) the surface was recooled to 120 K, (4) the surface was dosed a second time with the same amount of Rh(hfac)$(C_2H_4)_2$, and (5) TPR spectra were recorded at mass 63 as the surface was reheated. Desorption of Cu(hfac)$_2$ is enhanced when the surface is exposed to larger amounts of the precursor and also when the limiting surface temperature of the thermal cycling is low. The latter result may be surprising at first glance, but merely reflects the availability of hfac ligands, which in a competing process can fragment at higher temperatures. Similar results were obtained in our previous study of the reactions of Pd(hfac)$_2$ on Cu(111).[22,23]

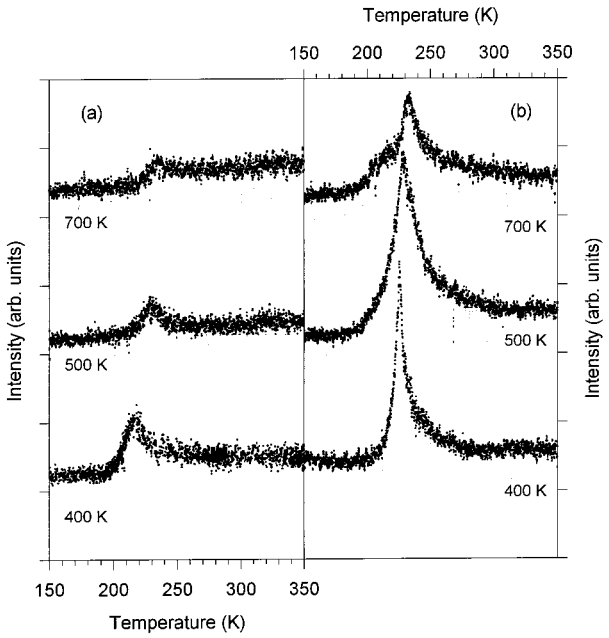

Figure 3. (a) TPR spectra ($m/e = 63$, Cu) of a 4 Θ_{sat} dose of Rh(hfac)$(C_2H_4)_2$ on Cu(111) following a 4 Θ_{sat} dose annealed to 400, 600, and 700 K and recooled to 120 K. (b) TPR spectra of a 8 Θ_{sat} dose of Rh(hfac)$(C_2H_4)_2$ on Cu(111) following a 8 Θ_{sat} dose annealed to 400, 600, and 700 K and recooled to 120 K.

Reactive Scattering of Rh(hfac)(C_2H_4) on Cu(111). The results in the last paragraph suggest that the transmetalation reaction that produces Cu(hfac)$_2$ should be favored when the surface is exposed to larger fluxes of Rh(hfac)$(C_2H_4)_2$. To test this hypothesis, we carried out reactive scattering experiments in which the products desorbing from the surface were monitored while the surface was exposed to a continual flux of Rh(hfac)$(C_2H_4)_2$ molecules. An effusive beam of the precursor was directed at the surface and the scattered flux detected at several selected masses as the temperature was raised and lowered at a constant rate (1 K s^{-1}). The masses examined included 26, 63, 69, and 103 (as appropriate for detecting C_2H_2, Cu, CF_3 and C_3O_2H, and Rh, respectively).

We see a steady scattering intensity following the mass 26 channel during both the heating and cooling cycles. At temperatures around 300 K, the cooling cycles show a decrease in intensity signifying condensation of the ethylene-containing fragment on the surface. Heating traces show the corresponding desorption feature for the mass 26 fragment.

The mass 103 channel tracks the scattering of Rh(hfac)$(C_2H_4)_2$ molecules off the surface; Figure 4 shows the results for one heating/cooling cycle. There is a marked conversion of Rh(hfac)$(C_2H_4)_2$ to other species at temperatures above 400 K, and this conversion is essentially quantitative above 600 K. Interestingly, the scattering wave forms show considerable hysteresis, with more Rh(hfac)$(C_2H_4)_2$ surviving its interaction with the surface during the cooling cycle. Repeating the heating/cooling cycle results in the same line shape and intensity of scattering. This result suggests that the surface becomes less reactive upon continued exposure to the Rh precursor. The reasons for this effect will be discussed below.

There are two principal pathways by which the Rh(hfac)$_2$-$(C_2H_4)_2$ precursor can react: transmetalation to give Cu(hfac)$_2$ and thermolysis to give hfac fragments. The contribution made by the former pathway can be inferred from an examination of the mass 63 trace taken during the reactive scattering experiment. The inset to Figure 4 shows a compilation of the data

(35) Girolami, G. S.; Jeffries, P. M.; Dubois, L. H. *J. Am. Chem. Soc.* **1993**, *115*, 1015−1024.

(36) Redhead, P. A. *Vacuum* **1962**, *12*, 203-211.

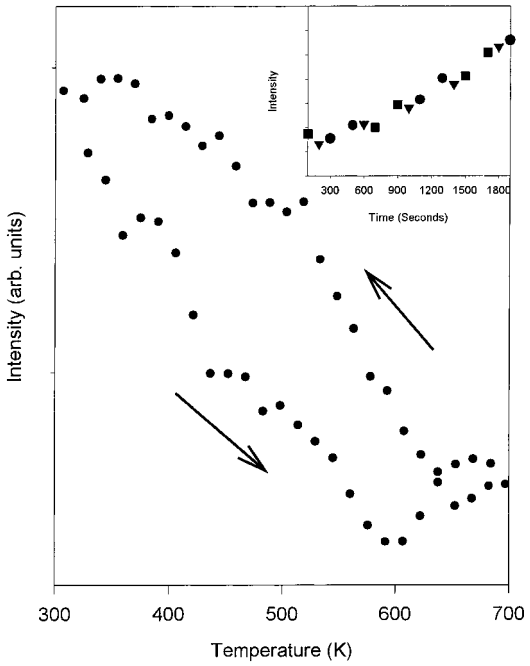

Figure 4. Profile obtained during the reactive scattering Rh(hfac)-$(C_2H_4)_2$ on Cu(111) tracking the desorption of Rh(hfac)$(C_2H_4)_2$ (m/e = 103). The heating rate was 1 K s^{-1}, and the arrows indicate whether the trace was obtained during the heating or cooling cycle. The inset depicts data obtained tracking the desorption of Cu(hfac)$_2$ (m/e = 63) as a function of time. The symbols correspond to temperatures 400 (■), 500 (▼), and 600 K (●).

measured at this mass over many scattering cycles. The data were extracted from the scattering profiles at three representative temperatures: 400, 500, and 600 K. For a reaction occurring solely via a transmetalation process, any decrease in rhodium scattering intensity should lead to a directly proportional increase in Cu(hfac)$_2$ production (branching with a process involving hfac ligand thermolysis should lead to an inhibition of the Cu-(hfac)$_2$ formation at temperatures above 600 K). The data in the inset to Figure 4 show that the Cu(hfac)$_2$ product flux does not follow the substrate temperature as we observed in the scattering studies above but increases progressively with the time of the exposure. The data in the inset were taken during the course of five temperature cycles alternating between heating and cooling with each shape in the figure denoting a representative temperature ((■) 400, (▼) 500, and (●) 600 K). As a function of temperature, the traces showed subtly increasing scattering intensity during heating cycles as well as a small condensation feature at low temperatures (∼350 K). The dominant trait, however, was the steadily increasing intensity with repeated cycling. Evidently, exposure of the surface to Rh-(hfac)$(C_2H_4)_2$ promotes the Cu(hfac)$_2$ etching process. This phenomenon may reflect the presence of increasing numbers of surface defects or (more likely) the presence of a surface alloy phase.

We have further probed how continued exposure of the surface to Rh(hfac)$(C_2H_4)_2$ affects the efficiency of the transmetalation process by performing a TPRS experiment immediately after a reactive scattering run. In this experiment, isothermal scattering was performed at various temperatures for 10 min with a flux of Rh(hfac)$(C_2H_4)_2$ equal to $\sim 4.2 \times 10^{11}$ molecules/(cm^2 s). After each run, the crystal was cooled to 120 K and dosed with Rh(hfac)$(C_2H_4)_2$ ($\sim 4\Theta_{sat}$), and the TPR spectrum was recorded at mass 63. The TPR spectra recorded after isothermal depositions carried out at 500, 600, 700, and 800 K are shown in Figure 5a−d, respectively.

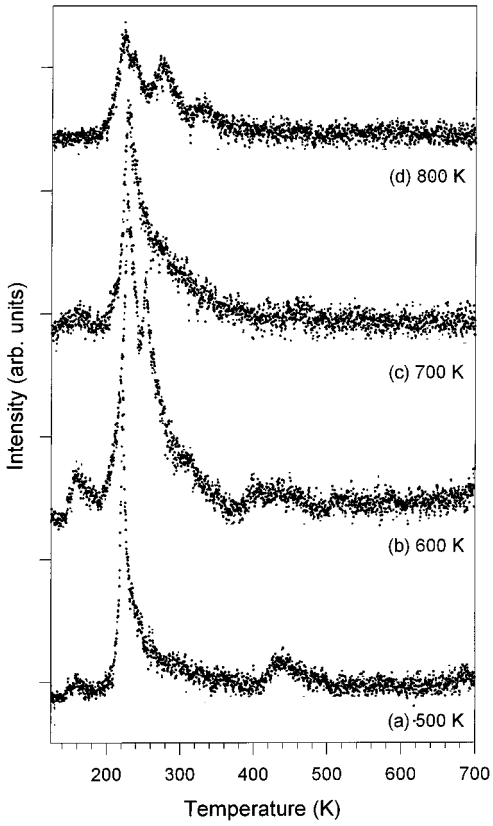

Figure 5. TPR spectra (m/e = 63, Cu) obtained after reactive scattering for 10 min at the temperatures indicated in the figure. The crystal was cooled to 120 K after the scattering and dosed with 4 Θ_{sat} prior to the taking of each TPR spectrum.

The influence of this thermal/chemical history on the formation of Cu(hfac)$_2$ is quite marked. Figure 5a, obtained after isothermal scattering at 500 K, shows a prominent TPRS peak for the production of Cu(hfac)$_2$ at 220 K; a smaller desorption peak is also seen at 420 K. These two features likely result from desorption-limited and reaction-limited rate processes, respectively. After scattering at 600 K (Figure 5b), we found a markedly enhanced production of Cu(hfac)$_2$, the majority of which desorbs to give two distinct peaks with maximums at ∼230 and 250 K. The definition of these peak maximums and the Cu(hfac)$_2$ yields are diminished when the prior scattering runs are conducted at higher temperatures, as seen in Figure 5c and d (which were performed at 700 and 800 K, respectively). The data suggest that exposure of the surface to Rh(hfac)$(C_2H_4)_2$ leads to a significant moderation of the mechanism(s) leading to Cu(hfac)$_2$ production.

Over the range of temperatures used, significant differences must exist in the nature of the ligand-derived debris present on the surface as well as the Rh/Cu compositional profile in the near-surface region (owing to interdiffusion of the deposited Rh into the copper substrate). AES data are consistent with this notion. Table 1 records the Rh:Cu ratios and the C:Cu ratios (corrected for AES sensitivity) taken after each isothermal scattering experiment. Between 400 and 500 K, the Rh:Cu ratio nearly doubles from 0.12 to 0.20. Above 500 K, however, the relative concentrations of the two metals remain essentially constant at ∼0.18. We know from the reactive scattering experiments that, above 500 K, the (thermolytic) reaction of Rh(hfac)$(C_2H_4)_2$ on Cu(111) under the conditions used here is approaching a flux-limited rate (a limiting behavior reached at ∼600 K). The AES results suggest that interdiffusion of Rh and Cu (which should become more rapid with increasing

Table 1. Surface Composition for Isothermal Scattering of $Rh(hfac)(C_2H_4)_2$ on Cu(111)[a]

temp, K	Rh:Cu ratio	C:Cu ratio
400	0.119	0.328
500	0.193	0.358
600	0.177	0.416
700	0.184	0.504

[a] For flux and time of surface exposure, see text. Composition ratios have been corrected for the differing sensitivities of the AES signals.

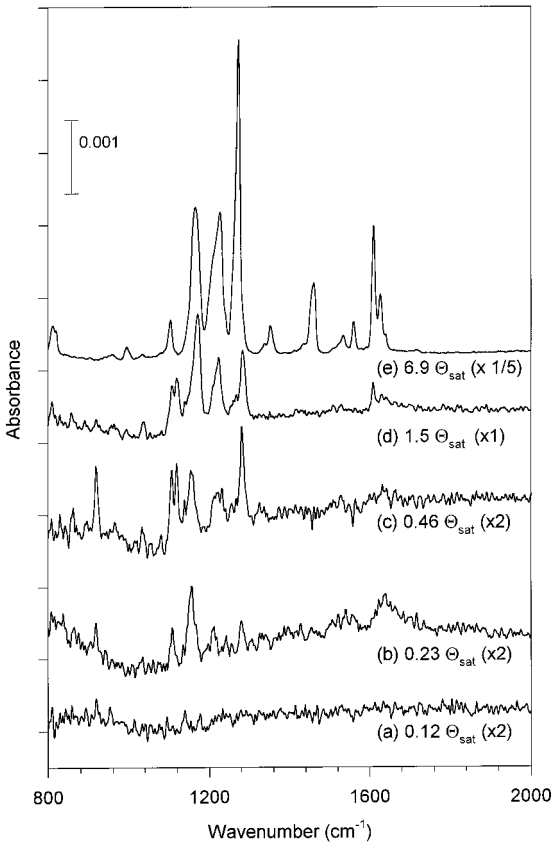

Figure 6. RAIR spectra of a clean Cu(111) single-crystal surface exposed to varying coverages of $Rh(hfac)(C_2H_4)_2$ at 100 K as indicated in the figure.

temperature) acts to maintain a constant near-surface composition—this suggests that a segregation effect operates in this system within these limits of temperature.

The C:Cu ratios measured by AES, however, behave quite differently. There is a marked increase in the carbon resident on the surface with increasing temperature. This carbon deposition may partly explain the inhibition effects seen for $Cu(hfac)_2$ production as revealed by the data presented in Figure 5.

RAIRS Studies of $Rh(hfac)(C_2H_4)_2$ on Cu(111). Reflection−absorption infrared spectroscopy (RAIRS) was used to investigate the structures of the adsorbates present on the surface at different precursor exposures and substrate temperatures. The experiments also examined the orientations and molecular organization of ligand-derived surface species. Figure 6 shows RAIR spectra recorded after exposure of the Cu(111) surface to coverages of $\sim$ 0.12, 0.23, 0.46, 1.5, and 6.9 Θ_{sat} $Rh(hfac)(C_2H_4)_2$ at 100 K. The peaks seen are in many ways similar to those observed for $Pd(hfac)_2$ and $Cu(hfac)_2$ deposited on a Cu(111) surface.[23,35] Peak assignments are made taking these previous studies into account and are summarized in Table 2.

At the lowest exposures ($\Theta \leq 0.23\ \Theta_{sat}$), six absorptions are seen. The feature at 918 cm^{-1} is assigned to a C−H bending mode for ethylene; this band is the primary IR active mode for ethylene π-bound to a copper surface.[37] In our system, it is not clear from the RAIR spectra whether the ethylene is bound to rhodium or copper, but the TPRS results (above) suggest that the $Rh(hfac)(C_2H_4)_2$ precursor readily transfers its ethylene ligands to the copper surface at low temperatures.

Table 2. Assignments of RAIR Spectrum of $Rh(hfac)(C_2H_4)_2$ on Cu(111) at 150 K

assignment	frequency, cm^{-1}
C═C stretch of hfac	1626
C═O stretch of hfac	1609
CO stretch + CH bend of hfac	1559, 1533
CCF_3 stretch of hfac	1461, 1351
CF_3 stretch of hfac (coupled with C═C?)	1272
CF_3 stretch of hfac (sym, in plane)	1223
CF_3 stretch of hfac (asym, out of plane)	1164
CH bend of hfac	1102
CH bend of ethylene	918

The spectra obtained at low exposures also show vibrational modes at 1117, 1164, 1219, 1283, and 1643 cm^{-1}, which correspond (predominantly) to the various modes of the hfac group as delineated in Table 2. At higher exposures ($\Theta \simeq 0.46\ \Theta_{sat}$), the intensities of these bands increase and an additional mode appears at 1106 cm^{-1}. Exposures larger than this lead to a marked increase in the relative intensity of the 1281 cm^{-1} mode. At saturation ($\Theta \geq 1.5\ \Theta_{sat}$ Figure 6d), strong, well-defined bands appear in the 1600 cm^{-1} region (most significant are the distinct peaks at 1607 and 1628 cm^{-1}).[38] These peaks have been assigned to the C═O stretch and the C═C stretch, respectively, and their appearance demonstrates that a significant number of the hfac ligands are oriented with the molecular plane perpendicular to the substrate.[39] The appearance of these modes is correlated with diminution of the characteristic ethylene peak at 918 cm^{-1}. We can therefore conclude that the precursor displaces the surface-bound ethylene derived from the dissociative adsorption of the $Rh(hfac)(C_2H_2)_2$ during dosing (we know from the TPRS studies that the binding energy of the ethylene is significantly less than that for the Rh complex and its nonethylene dissociative chemisorption fragments).

A multilayer of $Rh(hfac)(C_2H_4)_2$ gives a spectrum (Figure 6e) that is remarkably similar to that of $Pd(hfac)_2$ on Cu(111).[23,24] The mode assignments are summarized in Table 2.

Figure 7 shows the temperature dependence of the RAIR spectra. For each spectrum, the surface was exposed to a coverage $\Theta \simeq 1.5\ \Theta_{sat}$ of $Rh(hfac)(C_2H_4)_2$ at 100 K, and the surface was then heated briefly to a set temperature and finally recooled to 100 K. The presence of several C−F stretching bands suggests that the hfac groups adopt several different orientations at 100 K, much like they do in the multilayer (compare with Figure 6e). Annealing at 150 K (Figure 7b) gives a spectrum with vibrational modes essentially identical to those obtained without an annealing step (Figure 7a). The minor

(37) McCash, E. M. *Vacuum* **1990**, *40*, 423−427.

(38) Strong C═C and C═O stretching modes are seen at 1626 and 1609 cm^{-1}. Weaker peaks at 1560 and 1534 cm^{-1} are assigned to C−C stretches with some C−H bend contribution. The bands at 1461 and 1352 cm^{-1} are assigned to $C-CF_3$ stretching modes in analogy with the assignments for $Pd(hfac)_2$.[23,34] The strongest bands are those at 1272, 1223 and 1164 cm^{-1}. These peaks are all assigned to the C−F stretching motions for CF_3 groups of the hfac ligands. The features at 1223 and 1164 cm^{-1} are thought to be the in-plane and out-of-plane C−F stretches of the hfac ligand, respectively. The peaks at 1106 and 1157 cm^{-1} are tentatively assigned to CH bends from intact hfac ligands. Similar bands have been observed for $Pd(hfac)_2$ on Cu(111) (the 1109 cm^{-1} mode was not given a specific assignment in that study) and $Cu(hfac)_2$ on both a Cu(111) and Cu(100) surfaces.

(39) Woodruff, D. P.; Delchar, T. A. *Modern Techniques of Surface Science*; Cambridge University Press: New York, 1986.

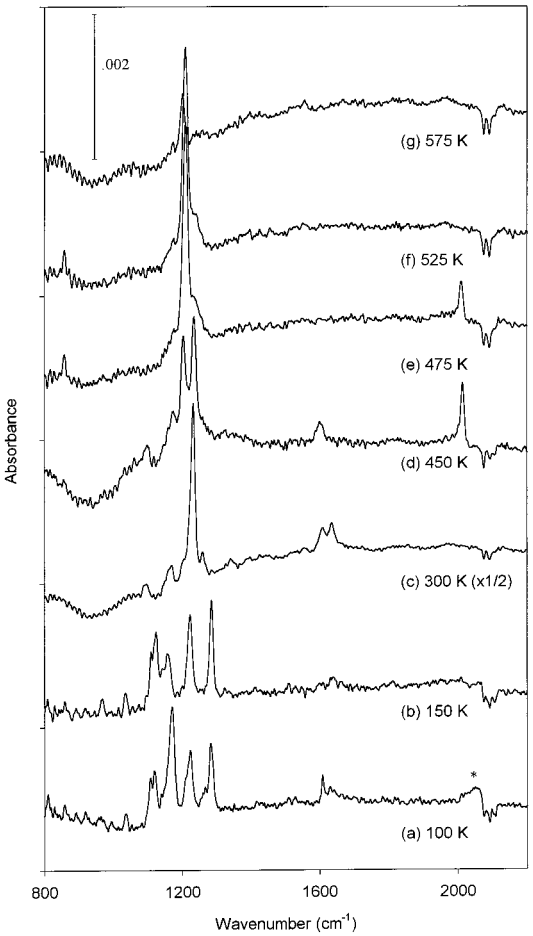

Figure 7. RAIR spectra of a clean Cu(111) single-crystal surface exposed to 1.5 Θ_{sat} of Rh(hfac)$(C_2H_4)_2$ at 100 K and annealed briefly to the indicated temperature. The feature marked by * in the $T = 100$ K spectrum results from an artifact from the reference spectrum.

changes in the band intensities indicate that there is some reordering upon heating (an increase in the intensity of the in-plane stretching mode and a decrease in that of the out-of-plane mode suggests that the hfac ligands adopt a slightly stronger average orientation along the surface normal direction).

Annealing to 300 K (Figure 7c) produces a dramatic change in the RAIR spectrum. The changes are very similar to those seen upon annealing Cu(111) surfaces dosed with Pd(hfac)$_2$ and Cu(hfac)$_2$ to this same temperature.[23,35] The spectrum obtained after this anneal is dominated by one main peak at 1235 cm^{-1}. We assign this band to an in-plane C−F stretch of a hfac ligand bound to the Cu(111) substrate. The presence of only one C−F stretching band in this spectrum clearly reveals that a tilt-ordering transition has occurred, one that aligns the plane of the hfac group perpendicular to the plane of the surface. This organizational state persists until the sample is heated past ∼350 K. Above this temperature, heating produces changes that are characteristic of the progressive thermal decomposition of the hfac group. The most notable change is the replacement of the 1235 cm^{-1} band by a weaker band at 1203 cm^{-1} (Figure 7d). This latter band is a diagnostic signature of surface-bound CF_3 groups.[35] These latter groups are relatively stable and persist to temperatures in excess of ∼575 K (Figure 7g). This decomposition also produces a transient mode at 2004 cm^{-1}; an earlier report assigned this feature to a ketenylidene species which appears to decompose itself at temperatures above ∼500 K).[35]

XPS Studies of Rh(hfac)$(C_2H_4)_2$ on Polycrystalline Copper. The transmetalation process resulting in the formation of

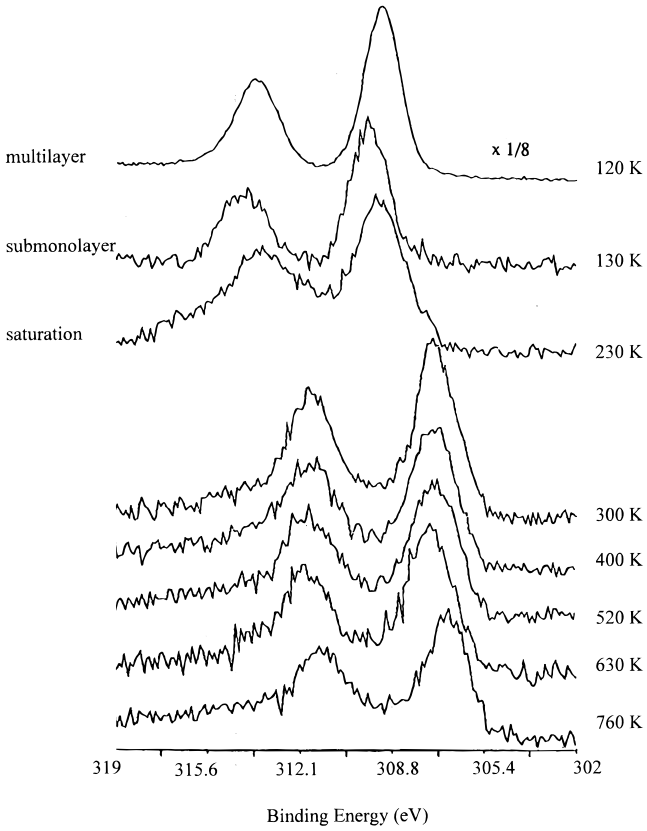

Figure 8. Rh 3d XP spectra of a clean polycrystalline copper surface exposed to Rh(hfac)$(C_2H_4)_2$ and annealed to the indicated temperature.

Cu(hfac)$_2$ is a redox process, and X-ray photoelectron spectroscopy is ideal for following changes in the oxidation state of the metal centers. In addition, XPS can give information about the chemical environments of the atoms in the hfac ligands and can probe whether the metal atoms generated from the precursor diffuse into the copper substrate. Owing to sampling constraints, a polycrystalline copper foil was used in these studies rather than a single crystal.[40,41] This substitution should increase the rate of diffusion of the deposited metal into the substrate (due to the increased number of grain boundaries) but should have only minor effects on reactions happening at the surface itself. All the binding energies were referenced to the Cu $2p_{3/2}$ peak (932.7 eV).

The top spectrum in Figure 8 shows the rhodium XPS data obtained from a multilayer of Rh(hfac)$(C_2H_4)_2$ deposited at 120 K. The rhodium binding energies, 314.1 eV (Rh $3d_{3/2}$) and 309.4 eV (Rh $3d_{5/2}$), are characteristic of the Rh^{I} oxidation state expected for the bulk precursor.[42,43]

The C 1s spectrum of the multilayer at 120 K (Figure 9) shows three distinct peaks at 293.2, 288.1, and 285.2 eV. The integrated intensities of these peaks are 2.4:1.6:5.0. Previous studies of hfac complexes show that these peaks can be assigned to the CF_3, C═O, and CH groups of the hfac ligand, respectively; the ethylene carbons should have a binding energy essentially identical with that due to the CH carbon of the hfac ligand.[23,35,44,45] The observed 2.4:1.6:5.0 intensity ratio differs

(40) Powell, C. J. *Crit. Rev. Surf. Chem.* **1993**, *2*, 17−35.
(41) Hercules, D. M. *Crit. Rev. Surf. Chem.* **1992**, *1*, 243−277.
(42) Anderson, S. L.; Watters, K. L.; Howe, R. F. *J. Catal.* **1979**, *59*, 340−356.
(43) Frederick, B. G.; Apai, G.; Rhodin, T. N. *J. Am. Chem. Soc.* **1987**, *109*, 4797−4803.
(44) Dubois, L. H.; Jeffries, P. M.; Girolami, G. S. In *Advanced Metalization for ULSI Applications*; Rana, V. S., Joshi, R. V., Ohdomari, I., Eds.; Materials Research Society: Pittsburgh, 1992; pp 375−382.

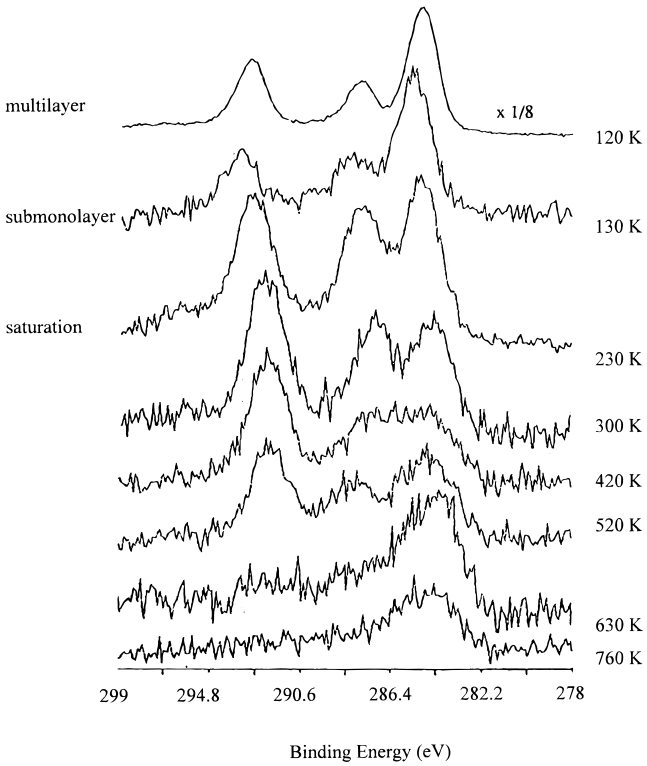

Figure 9. C 1s XP spectra of a clean polycrystalline copper surface exposed to Rh(hfac)$(C_2H_4)_2$ and annealed to the indicated temperature.

from the 2:2:5 ratio expected from the precursor because a shake-up peak related to the C═O $\pi \rightarrow \pi^*$ transition overlaps the feature due to the CF_3 carbon.[45] When the effect of the shake-up peak is taken into account, the spectra are consistent with the presence of intact precursor molecules. This observation is consistent with the TPR studies described above, which showed that the multilayer is stable below 220 K. The F 1s and the O 1s binding energies are consistent with those reported for other hfac-containing molecules.[23] These spectra are available as Supporting Information.

Submonolayer coverages of Rh(hfac)$(C_2H_4)_2$ on polycrystalline copper at 120 K give XP spectra that closely resemble those of a multilayer. The small differences in binding energies may be attributed to final state effects.[46] The binding energies of Rh^I and Rh^0 differ by ~2.5 eV, and these oxidation states are easily distinguished.[39] The observed XPS binding energy clearly shows that the copper surface is unable (either for thermodynamic or kinetic reasons) to reduce the metal center of the Rh^I compound at 120 K. This behavior contrasts dramatically with that seen for the palladium compound Pd$(hfac)_2$, which is reduced on copper surfaces to Pd^0 even at 110 K.[22−25]

We next examined XP spectra of submonolayers that had been briefly annealed at various temperatures and recooled to 120 K (Figure 8). These spectra provide information about irreversible, thermally driven reactions of the adsorbed species. When the surface is heated to 230 K (which is just above the measured multilayer desorption temperature), the Rh $3d_{5/2}$ peak becomes asymmetric and shifts by ~0.5 eV. The asymmetric line shape indicates that multiple species may be present; the shift to lower binding energy is consistent with a progressive dissociation of the ethylene ligands from the Rh^I centers. This latter suggestion is supported by the changes seen in the C, O, and F 1s spectra. Specifically, upon annealing the surface at 230 K, the CH_x peak diminishes so that the relative intensities of the CF_3:C═O:CH_x peaks are 2.4:1.6:3.0. These ratios suggest that the hfac ligand remains intact but that much of the ethylene has been lost. This conclusion is consistent with the TPR and RAIRS data, which indicate that the ethylene readily dissociates from the precursor and desorbs from the copper surface below this temperature.

When the dosed surface is heated to 300 K, the Rh $3d_{5/2}$ binding energy decreases dramatically to 307.0 eV, a value typical of metallic rhodium. The C 1s binding energies also change, but the relative intensities of the three peaks remain 2.4:1.6:3.0. Thus, on copper surfaces, reduction of the Rh^I center to Rh^0 has a relatively high activation barrier relative to that for the reduction of the Pd^{II} center in Pd$(hfac)_2$ to Pd^0. In all of these systems, the electrons needed for the reduction come from the copper crystal.

The reactions of the hfac groups at higher temperatures were studied by saturating the surface with Rh(hfac)$(C_2H_4)_2$ at 300 K, heating the surface to the desired temperature for 15 min, and then recooling the surface to 300 K. The resultant XP spectra show that the metallic rhodium atoms stay in the metallic state even to the highest temperature probed (800 K) but that the C, O, and F chemical environments change significantly. Specifically, the C 1s spectra show that the C═O peak decreases in intensity above 300 K and eventually disappears around 630 K. The CF_3 peak remains largely unchanged to 520 K (except for small shifts in binding energy) but also disappears by 630 K. Concomitant with these changes, a peak at ~284 eV (corresponding to amorphous or graphitic carbon) grows in and eventually dominates the spectra seen at high temperatures. The F and O 1s XPS signals become less intense and shift gradually to lower binding energies as the temperature is increased. At 760 K, the concentrations of fluorine and oxygen atoms on the surface are below the XPS detection limits. All of these observations suggest that the hfac ligands fragment above 300 K; this conclusion is consistent with studies of other hfac complexes (especially those of Cu)[23,35,44] and also with the TPR and RAIRS studies presented here.

The reduction of the Rh(hfac)$(C_2H_4)_2$ precursor generates rhodium atoms on the surface of the Cu(111) substrate. It is of interest to establish whether these metal atoms remain on the surface or diffuse into the bulk. To answer this question, we monitored the temperature dependence of the XPS signal due to the rhodium atoms generated by reduction of the rhodium precursor on a polycrystalline copper foil. No changes in the intensities of the Rh XPS peaks were noted up to 800 K. Even at this temperature, the signal intensities are unchanged after 3 h. The sample depth for the X-rays in this experiment is ~20 Å[47] and thus we can conclude that the rhodium atoms form a kinetically stable overlayer on the copper surface, a finding that is supported by the AES results described earlier. This behavior contrasts with that of the palladium atoms on polycrystalline copper foils: palladium atoms readily diffuse into the copper substrate within minutes at 623 K.[24]

TPRS Studies of Pt(hfac)$_2$ on Cu(111). Temperature-programmed reaction data for Pt$(hfac)_2$ on Cu(111) were obtained at masses 28, 50, 69, 195, and 63, which correspond to ions for the fragments CO, CF_2, CF_3 or C_3O_2H, Pt, and Cu, respectively. The data obtained from multilayer coverages in

(45) Cohen, S. L.; Liehr, M.; Kasi, S. *Appl. Phys. Lett.* **1992**, *60*, 50−52.

(46) Laibinis, P. W.; Bain, C. D.; Nuzzo, R. G.; Whitesides, G. M. *J. Phys. Chem.* **1995**, *99*, 7663−7676.

(47) Moulder, J. F.; Stickle, W. F.; Sobol, P. E.; Bomben, K. D. *Handbook of X-ray Photoelectron Spectroscopy*; Perkin-Elmer: Eden Prairie, MN, 1992.

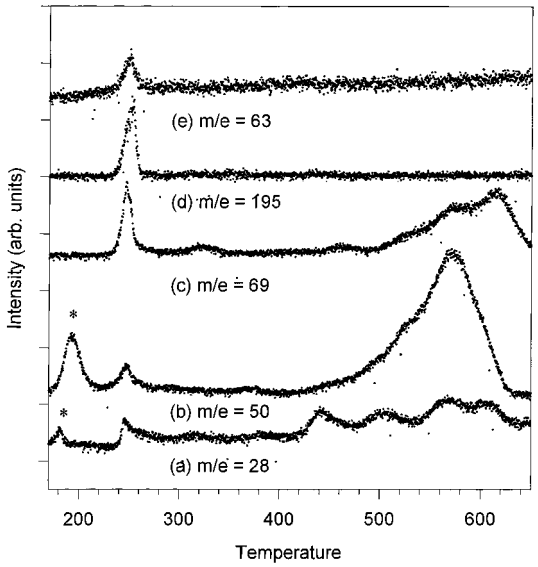

Figure 10. TPR spectra of a multilayer dose of $Pt(hfac)_2$ on a 150 K Cu(111) surface. Masses followed were $m/e = 28$ (CO), $m/e = 50$ (CF_2), $m/e = 69$ (CF_3 and C_3O_2H), $m/e = 195$ (Pt), and $m/e = 63$ (Cu) as indicated. The feature marked by * is a desorption feature of Hhfac introduced as a byproduct upon dosing with the $Pt(hfac)_2$.

the range of 1.5−3.0 θ_{sat} are shown in Figure 10a−e. The general features observed in the TPR spectra follow very closely those seen for hfac complexes of other late transition elements. Some quantitative differences are noted, however. The $Pt(hfac)_2$ multilayer desorption temperature is ∼250 K (we believe the feature seen below 200 K in Figure 10a and b results from a hexafluoroacetylacetone impurity in the sample flux which we were not able to eliminate completely). At temperatures above 400 K, the hfac groups begin to decompose, and these thermolysis reactions are essentially complete by 650 K.[23,35]

Small amounts of copper-containing species (presumably $Cu(hfac)_2$) also desorb from the surface. As shown in Figure 10e, a peak in the mass 63 channel is seen at 230 K. We believe this latter peak involves the desorption-limited evolution of $Cu(hfac)_2$; no reaction-limited $Cu(hfac)_2$ desorption processes are seen. The generation of $Cu(hfac)_2$ shows that some of the hfac groups dissociate at low temperatures from the Pt centers of the precursor.

If the TPRS experiments are performed multiple times without cleaning the surface between successive doses, the yield of $Cu(hfac)_2$ per dosing cycle steadily increases. To examine this point further, we carried out TPRS studies of surfaces that had been pretreated by exposing them to continuous fluxes of $Pt(hfac)_2$. In these studies, the Cu(111) surface was first exposed at a constant temperature to a $Pt(hfac)_2$ flux of 1.0×10^{11} molecules cm^{-2} s^{-1} for 10 min; the surfaces were then cooled, dosed at 150 K with an exposure equivalent to a coverage of ∼1.5 Θ_{sat} of $Pt(hfac)_2$, and then heated to obtain the TPRS data. The temperature at which the pretreatment was carried out has a marked effect on the Cu etching yields and energetics (Figure 11a−e). A desorption-limited peak at ∼230 K is seen irrespective of the pretreatment temperature. At pretreatment temperatures of 500 K and above, a second reaction-limited desorption process becomes progressively more important. A coverage-dependent study (data not shown) revealed that the higher temperature desorption process saturates first. Pretreating the surface increases the $Cu(hfac)_2$ yield by as much as 70%, the largest yield being seen for the 800 K treatment.

These data demonstrate a general pattern: the assembly and desorption of $Cu(hfac)_2$ molecules is promoted as the crystal is subjected to larger and larger integrated fluxes of the $Pt(hfac)_2$ precursor, and this effect is more pronounced at higher temperatures.

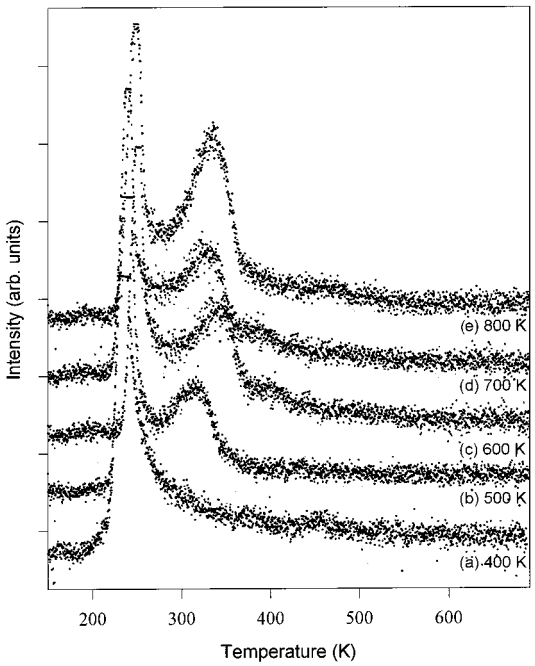

Figure 11. TPR spectra ($m/e = 63$) obtained after reactive scattering for 10 min at the indicated temperature. The crystal was cooled to 150 K after the scattering and dosed with ∼1.5 Θ_{sat} prior to the taking of each TPR spectrum.

Table 3. Assignments of RAIR Spectrum of $Pt(hfac)_2$ on Cu(111) at Various Temperatures[a]

assignment	100 K	175 K	250 K
C═C stretch			
C═O stretch	2085 (from impurity)	2085	1606
CO stretch + CH bend		1588	
CCF_3 stretch		1348	
CF_3 stretch (coupled with C═C?)	1293	1293	
CF_3 stretch (sym, in plane)	1224 (weak)	1228	1235
CF_3 stretch (asym, out of plane)	1178	1179	1173
CH bend			1099

[a] Frequencies of bands given in cm^{-1}.

RAIRS Studies of $Pt(hfac)_2$ on Cu(111). The RAIR spectra of $Pt(hfac)_2$ on Cu(111) are summarized in Table 3 along with relevant mode assignments. Again the position and nature of the vibrations follow closely those of the other β-diketonate compounds reported elsewhere.[23,35,44]

The temperature dependence of the RAIR spectra obtained at a coverage of $Pt(hfac)_2$ below saturation ($\Theta \simeq 0.8\ \Theta_{sat}$) is shown in Figure 12. The band at 1179 cm^{-1} seen in the 100 K spectrum (Figure 12a) is assigned to an out-of-plane C−F stretching motion of the hfac ligand. The presence of only one strong C−F stretching band strongly suggests that the $Pt(hfac)_2$ molecules adsorb molecularly at low temperature in an orientation coplanar with the surface. The spectrum stands in sharp contrast with those of other metal β-diketonate species, which at similar temperatures and coverages contain bands of comparable magnitude due to both in-plane and out-of-plane C−F stretching modes.[23,35]

Heating the $Pt(hfac)_2$-covered surface leads to substantial changes in this organizational architecture. For example, annealing to 175 K (Figure 12b) causes the emergence of a strong band at 1227 cm^{-1}. The presence of this band (which we assign

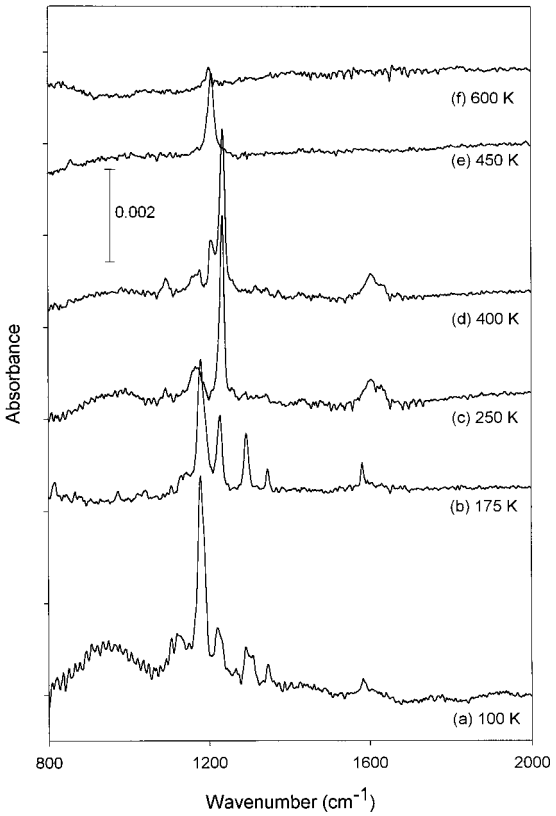

Figure 12. RAIR spectra of 0.8 Θ_{sat} doses of $Pt(hfac)_2$ on clean Cu-(111) 100 K surfaces briefly annealed to the indicated temperature.

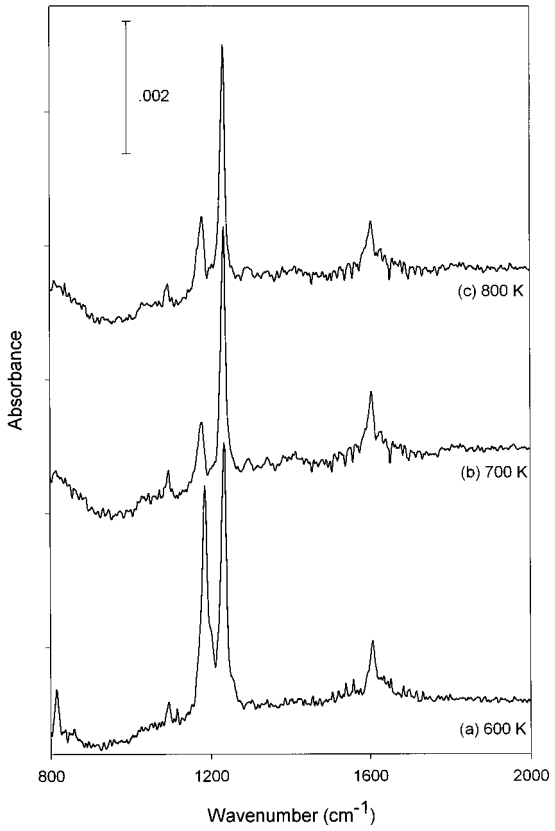

Figure 13. RAIR spectra of 1.5 Θ_{sat} doses of $Pt(hfac)_2$ on Cu(111) surfaces (175 K) previously dosed with 1.5 Θ_{sat} of $Pt(hfac)_2$ and annealed to the indicated temperature. All spectra were obtained at 175 K.

to an in-plane C−F stretch of intact hfac ligands) as a dominant component signifies a tilt-order transition of the hfac groups. The new state projects the hfac plane nearly perpendicular to that of the surface. This orientation becomes dominant when the sample is heated to 250 K (Figure 12c). We attribute this change in the orientation of the hfac groups to the transfer of these ligands from the Pt centers to the Cu surface.

Annealing at progressively higher temperatures (>400 K, Figure 12d) leads eventually to decomposition of the hfac groups. This reaction initially gives surface-bound CF_3 groups, species identifiable by their characteristic absorption at 1206 cm^{-1}.[35] The decomposition of the CF_3 groups becomes rapid above 500 K (as evidenced by the nearly featureless RAIR spectrum obtained after annealing the sample at 600 K, Figure 12e).

We have also used RAIRS to study why the desorption kinetics and yields of copper-containing products depend on the exposure history of the Cu surface. A clean copper surface at 175 K was first dosed with an exposure equivalent to a coverage of $\Theta \simeq 1.5\ \Theta_{sat}$ of $Pt(hfac)_2$. The sample was then annealed at a higher temperature for several seconds, recooled to 175 K, dosed with a monolayer of $Pt(hfac)_2$, and finally examined by RAIRS. The annealing temperatures used in the pretreatment step were 600, 700, and 800 K (Figure 13a−c, respectively). For the sample pretreated at 600 K (Figure 13a), two bands due to C−F stretching motions are seen at 1184 and 1234 cm^{-1} (these modes have some C−C stretching character also). This spectrum suggests a complex organization of hfac groups is present on the surface. Annealing this sample at 300 K yields a spectrum (data not shown) that is virtually identical to that obtained for an initially clean surface that was similarly dosed and annealed. In comparison, the spectra taken for samples pretreated at 700 and 800 K (Figure 13b and c) are remarkably simple. These latter spectra show the dichroism expected for essentially perpendicular orientations of the hfac groups relative to the surface. This result suggests that the pretreatment promotes the transfer of the hfac ligands from the $Pt(hfac)_2$ precursor to the surface. This inference was further supported by control experiments that clearly showed the limiting cycle temperature and not the time the crystal was held at 175 K after the second dose led to the differences evidenced in the data shown in Figure 13.

XPS Studies of $Pt(hfac)_2$ on Polycrystalline Copper. The reactions of $Pt(hfac)_2$ on copper foils were followed by XPS using the dosing and annealing protocols described in the Experimental Section.

For a multilayer of $Pt(hfac)_2$ at 150 K, the Pt $4f_{7/2}$ and $4d_{5/2}$ peaks appear at 74.4 and 317 eV, respectively[48] (upper spectrum in Figure 14). Both of these binding energies correspond to the Pt^{II} oxidation state.[41,49] The binding energies of the C, O, and F core levels are consistent with the presence of intact hfac groups on the surface at this temperature, as discussed in the rhodium XPS studies. The relative intensities of the CF_3, CO, and CH peaks in the C 1s spectrum (2.2:1.6:1.0 rather than the simple 2:2:1 ratio expected from the molecular stoichiometry) are affected by a shake-up peak for the C═O carbon, which overlaps with the CF_3 peak.[45]

The XPS spectrum of a submonolayer coverage of $Pt(hfac)_2$ shows that the molecules remain intact at 155 K. The binding energies are shifted by a few tenths of an electronvolt from those

(48) The Pt $4f_{7/2}$ peak cannot be used to determine the oxidation state of platinum for submonolayer amounts of $Pt(hfac)_2$, owing to interference from the Cu $3p_{3/2}$ peak at 77 eV. Therefore, the Pt($4d_{5/2}$) peak must be used to gauge the oxidation state of platinum.

(49) Escard, J.; Pontvianne, B.; Chenebaux, M. T.; Cosyns, J. *Bull. Soc. Chim. Fr.* **1975**, *112*, 2399−2402.

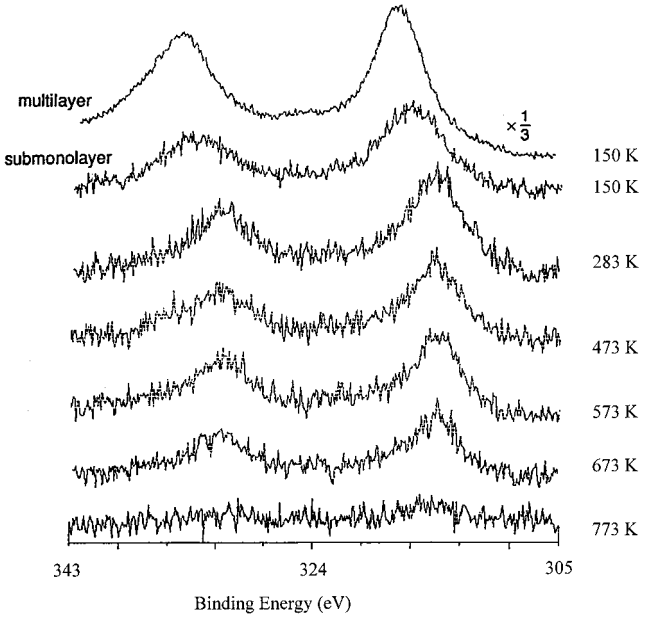

Figure 14. Pt 4d spectra of a clean polycrystalline copper surface exposed to $Pt(hfac)_2$ and annealed to the indicated temperatures. The heating rates were 2 K s^{-1} and all spectra were taken at 120 K.

seen for the multilayer. Again, we believe these differences are due to final state effects.[46] The shifts are not consistent with the reduction of the Pt^{II} centers to Pt^0.

The presence of intact $Pt(hfac)_2$ molecules on the copper surface at 150 K again stands in sharp contrast to the reactions observed for the palladium analogue $Pd(hfac)_2$, which is rapidly reduced by the copper surface to Pd^0 at temperatures as low as 120 K.[23]

Upon annealing the copper surface to temperatures between 150 and 283 K, the Pt $4d_{5/2}$ binding energy decreases steadily from 316.6 to 314.8 eV. For example, when a surface dosed with submonolayer amounts of $Pt(hfac)_2$ is annealed to 220 K, a broad Pt $4d_{5/2}$ peak appears at 315.6 eV. This result is consistent with the presence of a mixture of intact $Pt(hfac)_2$ molecules and metallic platinum on the copper surface.[23] The binding energies of the O 1s, C 1s, and F 1s core levels are also consistent with the presence of both intact $Pt(hfac)_2$ molecules and surface-bound hfac groups at this temperature.

When the surface is heated further to 283 K, the Pt $4d_{5/2}$ binding energy changes significantly, and the 314.8 eV value is consistent with complete reduction to the Pt^0 oxidation state.[49] The reduction process is most likely accompanied by transfer of the hfac ligands to the copper surface. The O 1s, C 1s, and F 1s spectra, all of which show further shifts of the core levels to lower binding energies, support this presumption. The most pronounced of the shifts is seen for the O 1s peak, which moves by 0.9 eV to lower binding energy when the hfac ligand transfer takes place. This substantial shift strongly suggests that the hfac ligands bind to the copper surface through their oxygen atoms.[23]

After the $Pt(hfac)_2$-dosed surfaces are annealed to 370 K, the C 1s, O 1s, and F 1s XP spectra show that most of the hfac ligands remain intact. At 473 K, however, the C 1s spectrum is dominated by a peak at 284.0 eV due to amorphous (or graphite-like) carbon. Minor peaks at 291.7 and 288.2 eV may be due to residual hfac ligands or fragments thereof. The O 1s spectrum contains a large peak at 532.1 eV, which we assign to surface-bound oxygen atoms. In addition, a peak is seen at 534.9 eV due to organic fragments derived from the hfac groups. Interestingly, the F 1s spectrum shows a new peak at 683.2 eV along with the peak due to the CF_3-containing fragments at 687.8 eV. This new peak can be assigned to fluoride atoms on the surface. This peak was not seen in the rhodium studies and we believe that it signals (at least in part) the cleavage of some of the C−F bonds by secondary electrons. When the surface is annealed to higher temperatures, graphitic carbon becomes the dominant surface species. The intensities of the peaks due to other surface species decrease significantly because most of the organic fragments desorb from the surface.

The intensities of the Pt 4d peaks decrease as the surface is annealed to higher temperatures. These peaks are no longer detectable when the surface is heated to 773 K for 60 s. The sampling depth for platinum is dictated by the mean free path (λ) of its photoelectrons, which is ~20 Å for photoelectrons of this kinetic energy.[47] Because no platinum-containing species have desorbed from the surface (as we saw from the TPR studies), this result suggests that the platinum atoms have diffused substantially into the bulk. Attenuation of Pt $4d_{5/2}$ core level emission to the noise-limited level is expected to occur at a diffusion length of the order of ~2λ. Thus, in 1 min, the Pt atoms must diffuse at least ~40 Å into the Cu substrate at this temperature. These results, which were obtained on a Cu polycrystal, are similar to those obtained in AES studies made on a Cu(111) single crystal.

Discussion

We have previously described our discovery of an interesting chemical vapor deposition process that constitutes a method for effecting surface-selective metallization by palladium.[22−25] At temperatures below 400 °C and in the absence of an external reductant such as H_2, the palladium(II) hexafluoroacetylacetonate complex $Pd(hfac)_2$ deposits palladium selectively on copper (and iron) substrates, but not on silicon, silicon dioxide, or several other substrate materials. Our studies demonstrated that the metallization process takes place by means of a redox transmetalation reaction, in which the deposition of palladium occurs simultaneously with etching of the copper surface.[22−25] In the course of this process, Cu^0 reacts with Pd^{II} to afford Cu^{II} and Pd^0, and the hfac ligands are transferred from palladium to copper.[50] The overall reaction is as follows:

$$Pd(hfac)_2 + Cu \rightarrow Cu(hfac)_2 + Pd \qquad (a)$$

The driving force for this reaction was proposed to be the thermodynamics of the redox event: standard electrochemical potentials show that copper(0) reduces palladium(II) but not vice versa. Support for the hypothesis that the reaction is thermodynamically driven comes from the observation that the reverse redox transmetalation reaction, i.e., the reaction of $Cu(hfac)_2$ with Pd metal to give Cu and $Pd(hfac)_2$, does not take place to any significant degree.

Our mechanistic studies of the deposition of Pd from $Pd(hfac)_2$ on copper surfaces showed that four different intimate steps were involved: (1) adsorption of $Pd(hfac)_2$ on the surface, (2) reduction of the precursor to Pd metal and simultaneous transfer of the hfac groups to the copper surface, (3) assembly and desorption of the $Cu(hfac)_2$ product, and (4) interdiffusion of the Pd atoms into the bulk of the copper substrate and transport of fresh copper atoms to the surface. The last of these steps ensures that the transmetalation process is a sustained one.

An interesting question to address is whether the palladium-on-copper system is unique or whether it is the first representa-

(50) A similar redox transmetalation reaction is used to deposit tungsten on silicon: WF_6 reacts with the Si substrate to afford W and SiF_4. Wang, J.-T.; Cao, C.-B.; Wang, H.; Zhang, S.-L. *J. Electrochem. Soc.* **1994**, *141*, 2192−2198.

tive of an entire class of surface-selective metallization processes. If the deposition of Pd on Cu is in fact driven thermodynamically, then it should be possible to predict whether other metal-on-metal depositions are or are not favorable simply by inspection of the relevant electrochemical half-cell potentials. For example, examination of such potentials shows that copper metal is able to reduce several transition metal cations (besides Pd^{II}) to the zero oxidation state. Among these cations are Rh^{I} and Pt^{II}, and at 25 °C the standard cell potentials for the $Rh/Rh^{+}//Cu^{2+}/Cu$ and $Pt/Pt^{2+}//Cu^{2+}/Cu$ redox couples are 0.42 and 0.84 V, respectively.[51] For comparison, the cell potential for the $Pd/Pd^{2+}//Cu^{2+}/Cu$ couple is 0.58 V, so that the Rh^{I} cell has a slightly smaller (but still favorable) driving force and the Pt^{II} cell a significantly larger driving force than the palladium/copper system. Although the electrochemical potentials given are those measured for standard aqueous conditions, we believe that the driving forces for the CVD reactions should follow the same order, especially if the precursors used are hfac complexes. Both water and hfac ligate to metal centers by means of oxygen atoms, and thus the d orbitals on the metal center should be of comparable energy. As a result, we would expect that the half-cell potentials of an ion surrounded by water molecules and that same ion surrounded by hfac ligands should be correlated in a predictable and systematic fashion. We therefore predicted that hfac complexes of Rh^{I} and Pt^{II} should engage in redox transmetalation reactions with copper surfaces.

Both Rh^{I} and Pt^{II} form stable, volatile coordination complexes with the hfac ligand. For Rh^{I}, we chose the ethylene complex $Rh(hfac)(C_2H_4)_2$ because it is simple to prepare, is convenient to handle at room temperature, and has a relatively high vapor pressure. The ethylene ligands will stabilize the Rh^{I} oxidation state and thus lower the driving force for reduction to Rh metal, but this effect should be moot under CVD conditions because the ethylene ligands should readily dissociate. For Pt^{II}, we chose the binary complex $Pt(hfac)_2$.

We expected these two complexes to serve as surface-selective CVD precursors by means of the following redox transmetalation reactions:

$$2Rh(hfac)(C_2H_4)_2 + Cu \rightarrow Cu(hfac)_2 + Rh + 4C_2H_4 \quad (b)$$

$$Pt(hfac)_2 + Cu \rightarrow Cu(hfac)_2 + Pt \quad (c)$$

In practice, no deposition of rhodium from $Rh(hfac)(C_2H_4)_2$ occurs on copper at temperatures below 200 °C, when H_2 is absent. Above this temperature, rhodium films are generated but the deposition process proceeds by means of a different reaction involving disproportionation of the Rh^{I} precursor to Rh metal and the Rh^{III} product $Rh(hfac)_3$.[26] For $Pt(hfac)_2$, no deposition of Pt occurs on copper surfaces in the absence of H_2, even at temperatures as high as 700 K. In neither system were detectible amounts of $Cu(hfac)_2$ produced. The present mechanistic investigation was undertaken to discern why the chemistry of these precursors differs so unexpectedly from that of $Pd(hfac)_2$.

Chemistry of the Precursors below 300 K. Summaries of the reactions of $Rh(hfac)(C_2H_4)_2$ and $Pt(hfac)_2$ on Cu(111) surfaces are given in Schemes 1 and 2. Scheme 1 shows that, at the lowest temperatures (<120 K), $Rh(hfac)(C_2H_4)_2$ adsorbs molecularly on the surface. Near 160 K, the ethylene ligands begin to dissociate from the Rh centers and desorb from the surface. Warming the surface to ~190 K causes the complete desorption of all of the ethylene molecules. Addition of excess $Rh(hfac)(C_2H_4)_2$ also promotes desorption of the ethylene groups and gives rise to a surface decorated with Rh(hfac) units. When the surface is heated to 230 K, the Rh^{I} centers begin to reduce to Rh^{0}, and the hfac ligands begin to transfer to the copper substrate. By 300 K, this tranformation is complete. The copper-bound hfac ligands are oriented with their molecular planes perpendicular to the plane of the surface.

Scheme 1

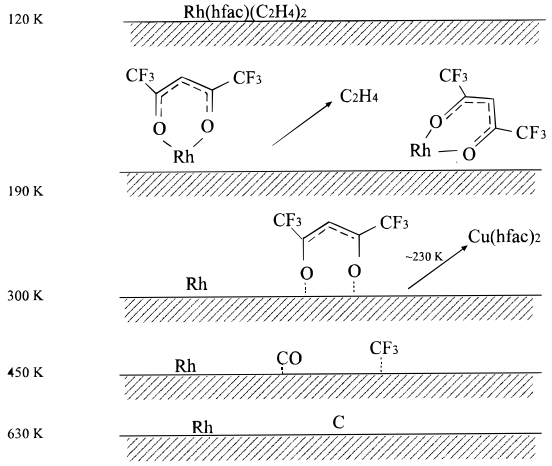

Scheme 2

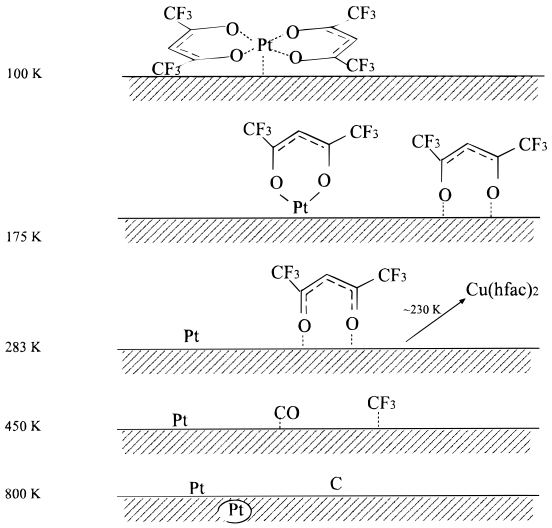

For the $Pt(hfac)_2$ precursor, the low-temperature chemistry is different but the same final state, zero-valent metal atoms and copper-bound hfac ligands, is generated at 300 K. Scheme 2 shows that, below 175 K, the molecule adsorbs intact with its plane parallel to the Cu(111) surface. Near 220 K, reduction of the metal center from Pt^{II} to Pt^{0} and the hfac ligands transfer to the copper surface. By 283 K, this process is complete. Again, the copper-bound hfac ligands are oriented with their molecular planes perpendicular to the plane of the surface.

The chemistry of $Rh(hfac)(C_2H_4)_2$ and $Pt(hfac)_2$ on Cu(111) differs from that of $Pd(hfac)_2$ in one key respect: whereas the former two molecules adsorb intact at temperatures below 175 K and are reduced to metal only above 200 K, the palladium complex loses its hfac ligands and is reduced to Pd^{0} even at 110 K. We suggest that the temperature at which the hfac ligands transfer to the copper surface (and the metals are reduced the zero-valent state) reflects the kinetic barrier for ligand dissociation. It is well known that the barrier for the exchange of oxygen

(51) Harris, D. C. In *Quantitative Chemical Analysis*, 3rd ed.; Freeman: New York, 1991; pp AP34−AP43.

ligands attached to Pt is much higher than that for the exchange of oxygen ligands attached to Pd: for example, water exchange in the tetraaquaplatinum(II) cation, $Pt(H_2O)_42^+$, is $\sim 1.4 \times 10^6$ times slower than that in $Pd(H_2O)_4^{2+}$.[52] If dissociation of the hfac ligands is the rate-determining step for the redox process, then the higher activation barriers for the reduction of the Pt precursor by copper (versus the reduction of the Pd precursor by copper) can be understood. This line of reasoning suggests a similar kinetic barrier underlies the Rh rate behaviors as well.

The difference in the temperature at which the hfac-transfer/metal-redox step occurs, however, is not likely to be responsible for the differing behavior of these three precursors under CVD conditions, for the simple reason that this step has a low barrier and is not rate-determining. Instead, the origin of the different CVD behavior must lie in subsequent steps, and we turn to a discussion of the evolution of the state seen for all three systems at 300 K: a copper surface decorated with zero-valent metal atoms and oxygen-bound hfac groups.

Chemistry of the Precursors above 300 K. At low surface coverages, such as those generated by dosing the Cu surface once with a monolayer of precursor, the principal chemistry seen at temperatures above 300 K is unimolecular fragmentation of the hfac groups. This process becomes rapid above 400 K. Among the species formed are surface-bound CF_3 groups, which eventually decompose or desorb into the gas phase above 500 K. Essentially identical fragmentation behavior is seen for the palladium, rhodium, and platinum systems.

For both the Rh and Pt systems, small amounts of $Cu(hfac)_2$ are formed when a clean surface is dosed once and then heated. If the surface is dosed and heated multiple times without cleaning the surface between successive doses, the yield of $Cu(hfac)_2$ per dosing cycle steadily increases (but still remains small). In addition, for the Pt system, increasing the Pt content of the surface leads to the emergence of a second, higher-temperature $Cu(hfac)_2$ desorption process, implying that at least some of the desorbing $Cu(hfac)_2$ originates from a surface, such as a copper/platinum alloy, with a binding energy that differs from that of pure copper.

The formation of an alloy by reaction of the $Pt(hfac)_2$ precursor with the copper surface is further demonstrated by differences in the orientation of $Pt(hfac)_2$ molecules adsorbed on a Pt-decorated Cu surface as opposed to a clean Cu surface. When significant quantities of Pt are present, the hfac groups align perpendicular to the surface (thus implying that the hfac ligands have dissociated from the $Pt(hfac)_2$ precursor); on the clean copper surface the hfac groups are aligned parallel to the surface (consistent with the presence of intact $Pt(hfac)_2$ molecules). We do not understand at present the microscopic basis by which the copper/platinum alloy promotes the dissociation of the $Pt(hfac)_2$ and related formation of $Cu(hfac)_2$.

Low surface coverages, however, are not characteristic of CVD processes, which are carried out in the presence of a significant vapor pressure of precursor at elevated temperature. In particular, the assembly of $Cu(hfac)_2$ is intrinsically an associative process, one that is promoted at high surface coverages.[24,25] To obtain high surface coverages in a UHV environment, we studied the reactions that occur in the presence of a constant flux of precursor molecules to the surface.

Under reactive scattering conditions, we observe a decrease in the production of $Cu(hfac)_2$ when the thermolysis rate of the $Rh(hfac)(C_2H_4)_2$ precursor is high (i.e., at high temperatures). Under such conditions, significant amounts of rhodium (and other products) are deposited on the surface but little time is permitted for diffusion. When sufficient time is allowed for diffusion, however, the overall rate of $Cu(hfac)_2$ production increases as a function of time or total coverage. This result implies that the alloying of copper and rhodium exhibits a slight promoter effect on $Cu(hfac)_2$ production.

For the rhodium complex under CVD conditions, where the fluxes and surface coverages are high, deposition of rhodium metal proceeds by means of a disproportionation mechanism in which $Rh(hfac)(C_2H_4)_2$ gives Rh metal, ethylene, and the rhodium(III) product, $Rh(hfac)_3$.[26] We have not been able to mimic this disproportionation reaction in a UHV environment, a result that suggests a strong (possibly non-first-order) weighting of the adsorbate coverage in the power rate law for the reaction.

Reasons for the Nonproduction of $Cu(hfac)_2$. The abstraction of copper atoms from the surface and formation of $Cu(hfac)_2$ is kinetically disfavored when Rh and Pt are present on the surface, but not when Pd is present. We believe that the different $Cu(hfac)_2$ yield seen for Rh and Pt on one hand, and Pd on the other, reflects the fate of the deposited metal atoms. At low temperatures, where the ligand thermolysis rates are slow, Rh and Pt diffuse slowly into copper and form stable overlayers. It is possible that the surface-bound hfac groups are unable to abstract a copper atom from the Rh- or Pt-covered surface; this inability would explain why $Rh(hfac)(C_2H_4)_2$ and $Pt(hfac)_2$ do not engage in sustained redox transmetalation reactions with copper. At high temperatures, interdiffusion processes will generate alloys. These alloys promote the transmetalation reaction, particularly in the case of the platinum alloy although the yield of the $Cu(hfac)_2$ that we have been able to obtain in this way is still small. In contrast, the rapid diffusion of palladium atoms into copper generates a copper-rich surface composition that can continue to react with $Pd(hfac)_2$ to form $Cu(hfac)_2$ in a kinetically competent process.

One of the primary differences in the metals is the rate of metallic interdiffusion. We demonstrated in the XPS studies that the diffusion into the bulk of the copper substrate is more rapid for platinum than for rhodium, but both processes are slower than diffusion of palladium into copper.[24] These findings are consistent with a limited database on the low-temperature diffusion coefficients for these combinations of metals.[53] At 843 K, a diffusion coefficient of $\sim 3.8 \times 10^{-11}$ cm^2 s^{-1} has been measured for palladium in a copper single crystal, 2.36×10^{-11} cm^2 s^{-1} for diffusion of platinum in a polycrystalline copper foil, and $\sim 2 \times 10^{-11}$ cm^2 s^{-1} for rhodium in a polycrystalline copper foil. The larger number of grain boundaries in foils generally leads to diffusion coefficients that are orders of magnitude faster than those found in the single crystals of the same substrate.[53] Hence, under identical circumstances, the interdiffusion for Pt and Rh with Cu is dramatically slower than interdiffusion of Pd and Cu.

The slower rate of diffusion will affect the rate of transmetalation. If the second metal (Pt, Rh, or Pd) is not incorporated into the bulk, we should observe a decrease in the production of $Cu(hfac)_2$ because the surface copper sites will be covered with the deposited metal and thus unavailable for reaction. Although redox transmetalation reactions do occur with the Pt and Rh reagents, they are quickly self-poisoning. Interdiffusion of these latter two metals into the copper substrate (and transport of fresh copper atoms to the surface) appears to be too slow to permit the formation of $Cu(hfac)_2$ to be kinetically competent.

(52) Helm, L.; Elding, L. I.; Marbach, A. E. *Inorg. Chem.* **1985**, *24*, 1719−1721.

(53) Butrymowicz, D. B.; Manning, J. R.; Read, M. E. *J. Phys. Chem. Ref. Data* **1976**, *5*, 103−200.

It is important to note that the slow kinetics of this latter rate process, while mirroring the reference data in the literature, may not reflect an intrinsic transport limit. The ligand decomposition processes, which compete with the reactive etching of copper, generate a carbonaceous overlayer. This adlayer could also limit the reactivity (by substantially lowering the reactive sticking probability of the precursors or by pinning the platinum or rhodium atoms at the growth surface). If these latter effects play an important role, we have not been able to demonstrate it conclusively. Indeed, the RAIRS experiments show hfac ligand coverages that only weakly correlate with the exposure history under the conditions used here. For this reason, it seems likely to us that the source of the transport limits implicated here for the platinum and rhodium cases are ones related to the intrinsic rates of diffusion in the solid state.

Acknowledgment. We thank the National Science Foundation (Grant CHE 9626871) and the Department of Energy through the University of Illinois at Urbana−Champaign Frederick Seitz Materials Research Laboratory (Grant DEFG 02-91-ER45439) for support of this work. We also thank Rick Haas for help with the XPS measurements.

Supporting Information Available: F 1s and O 1s XP spectra exposed to Rh(hfac)(C_2H_4)$_2$ and annealed to several temperatures (PDF). This material is available free of charge via the Internet at http://pubs.acs.org.

JA993653S